Chemosphere 108 (2014) 343–352

Contents lists available at ScienceDirect

Chemosphere

journal homepage: www.elsevier.com/locate/chemosphere

Comparative toxicity of silver nanoparticles on oxidative stress and DNA damage in the nematode, *Caenorhabditis elegans*

Jeong-Min Ahn [a,c,1], Hyun-Jeong Eom [a,c,1], Xinyu Yang [b], Joel N. Meyer [b], Jinhee Choi [a,c,*]

[a] School of Environmental Engineering, University of Seoul, Seoul 130-743, Republic of Korea
[b] Nicholas School of the Environment and Center for the Environmental Implications of Nanotechnology, Duke University, Durham, NC, USA
[c] Graduate School of Energy and Environmental system Engineering, University of Seoul, Seoul 130-743, Republic of Korea

HIGHLIGHTS

- $AgNO_3$ and bare AgNPs have similar toxicities whereas PVP-coating reduces the toxicity.
- Different responses of mutants suggest the distinct toxic mechanism of $AgNO_3$ and AgNPs.
- $AgNO_3$ and AgNPs induce oxidative stress-related mitochondrial DNA damage.

ARTICLE INFO

Article history:
Received 16 September 2013
Received in revised form 25 January 2014
Accepted 30 January 2014
Available online 13 April 2014

Handling Editor: Tamara S. Galloway

Keywords:
Silver nanoparticles
Caenorhabditis elegans
Comparative toxicity
Mitochondrial toxicity
Oxidative DNA damage

ABSTRACT

This study examined the effects of polyvinylpyrrolidone (PVP) surface coating and size on the organismal and molecular toxicity of silver nanoparticles (AgNPs) on the nematode, *Caenorhabditis elegans*. The toxicity of bare AgNPs and 8 and 38 nm PVP-coated AgNPs (PVP8-AgNPs, PVP38-AgNPs) were compared. The toxicity of $AgNO_3$ was also tested because ion dissolution and particle-specific effects are often important characteristics determining Ag nanotoxicity. Comparative toxicity across $AgNO_3$ and the three different types of AgNPs was first evaluated using a *C. elegans* mortality test by a direct comparison of the LC_{50} values. Subsequently, mutant screening followed by oxidative stress, mitochondrial toxicity and DNA damage assays were carried out at equitoxic (LC_{10} and LC_{50}) concentrations to further assess the toxicity mechanism of $AgNO_3$ and AgNPs. $AgNO_3$ and bare AgNPs had similar toxicities, whereas PVP coating reduced the toxicity of the AgNPs significantly. Of the PVP-AgNPs, the smaller NPs were more toxic. Different groups of mutants responded differently to $AgNO_3$ and AgNPs, which indicates that their toxicity mechanism might be different. $AgNO_3$ and bare AgNPs induced mitochondrial membrane damage. None of the silver materials tested caused detectable polymerase-inhibiting DNA lesions in either the nucleus or mitochondria as measured by a quantitative PCR assay, but $AgNO_3$, bare AgNPs and PVP8-AgNPs induced oxidative DNA damage. These results show that coatings on the AgNPs surface and the particle size make a clear contribution to the toxicity of the AgNPs, and oxidative stress-related mitochondrial and DNA damage appear to be potential mechanisms of toxicity.

1. Introduction

Silver nanoparticles (AgNPs), which have well-known antimicrobial properties, are used extensively in a range of medical and general applications (Varaprasad et al., 2011; Croes et al., 2012). Therefore, the toxicity of AgNPs has been investigated widely in many *in vitro* (Lamb et al., 2010; Shavandi et al., 2011; Mukherjee et al., 2012) and *in vivo* models (Sung et al., 2011; Wu and Zhou, 2012; Oukarroum et al., 2012). From these studies, the (cyto)toxicity of AgNPs has been attributed to many possible mechanisms, including the dissolution or release of Ag ions from the nanoparticles, oxidative stress, protein or DNA damage and apoptotic cell death (Arora et al., 2008, 2009; Gopinath et al., 2010; Hsin et al., 2008; Kim et al., 2009; Navarro et al., 2008). The mechanism of toxicity is likely to be dependent on the properties of the nanoparticles, such as the surface area, size and shape, capping agent, surface charge, and purity of the particles, structural distortion, and bioavailability of the individual particles (Jiang et al., 2009; Fubini et al., 2010; Tantra et al., 2010).

Although AgNPs have been applied widely in a range of fields using different formulations, the precise mechanisms of toxicity

* Corresponding author at: School of Environmental Engineering, University of Seoul, Seoul 130-743, Republic of Korea. Tel.: +82 2 2210 5622; fax: +82 2 2244 2245.
E-mail address: jinhchoi@uos.ac.kr (J. Choi).
[1] These authors contributed equally.

http://dx.doi.org/10.1016/j.chemosphere.2014.01.078
0045-6535/

of AgNPs with surface modifications are unclear. Only limited information is available on the comparative toxicity of coated vs. bare AgNPs (Shoults-Wilson et al., 2011; Ivask et al., 2014), or on different sized AgNPs (Park et al., 2011; Kim et al., 2012). Information on the comparative toxicity across different forms and sizes of AgNPs would help to develop a strategy for the safe application of AgNPs. Another knowledge gap on AgNPs toxicity appears to be genotoxicity. As oxidative stress has been studied as a mechanism of the toxicity of AgNPs, the studies on closely-related genotoxic potential are of increasing interest (Ahamed et al., 2008; Eom and Choi, 2010; Foldbjerg et al., 2011; Hackenberg et al., 2011; Asare et al., 2012; Nymark et al., 2013). However, information on the potential genotoxicity of AgNPs in *in vivo* models is still very much limited (Kim et al., 2008; Demir et al., 2011; Tiwari et al., 2011).

The nematode *Caenorhabditis elegans* has been a useful model for (environmental) toxicology (Leung et al., 2008), and more recently has been increasingly used for nanotoxicology (Zhao et al., 2013; Choi et al., 2014). This is due to its high degree of molecular conservation and the outstanding molecular, genetic, and genomic tools available, which provide mechanistic insights into human health effects. In our previous study, we investigated AgNPs induced oxidative DNA damage and repair in the nematode *C. elegans*, and found that bare AgNPs induced oxidative DNA damage and repair in a *pmk-1* dependent manner (Chatterjee et al., 2014). In a continuation of that study, here we extended genotoxicity tests to polyvinylpyrrolidone (PVP)-coated AgNPs. The comparative toxicity of bare AgNPs and two different sized PVP coated AgNPs (8 nm, referred as PVP8-AgNPs and 38 nm, referred as PVP38-AgNPs) were investigated. In addition, the toxicity of $AgNO_3$ was also examined by comparing the toxicity of the AgNPs and Ag ions to determine if the observed toxicity was due to dissolution or was particle specific because this determination is the most important characteristic for determining the nanotoxicity of Ag (Cong et al., 2011; van der Zande et al., 2012; Hoheisel et al., 2012; Yang et al., 2012; Eom et al., 2013). The comparative toxicity across $AgNO_3$ and three different types of AgNPs was first evaluated using a *C. elegans* mortality test by a direct comparison of the LC_{50} values. Subsequently, a mutant screening test followed by oxidative stress, mitochondria and DNA damage assays were carried out at the toxic equivalent concentrations (i.e. LC_{10} and LC_{50}) to further assess whether the toxicity mechanisms of $AgNO_3$ and three types of AgNPs are distinct or common in *C. elegans*, with special attention to DNA damage.

2. Materials and methods

2.1. Silver nanoparticles and physicochemical characterization

Suspensions of bare AgNPs (size <100 nm, Chemical, St. Louis, MO) were prepared in deionized water and dispersed by sonication for 13 h (Branson-5210 sonicator, Branson Inc., Danbury, CT, USA), stirring for 7 days, and filtering through a cellulose membrane (pore size 100 nm, Advantec, Toyo Toshi Kaisha, Japan) (Roh et al., 2009). PVP-coated AgNPs (PVP8 and PVP38) were manufactured at Duke University, as previously described (Yang et al. 2012). To compare the toxicities of AgNPs and Ag ions, aqueous $AgNO_3$ (AG002, Next Chimica, Centurion, Republic of South Africa) in deionized water (DW) was used and the final concentrations of AgNPs and $AgNO_3$ were verified using multitype inductively coupled plasma emission spectrometer (ICPE-9000, Shimadzu, Tokyo, Japan). The concentrations for AgNPs and $AgNO_3$ were in an equivalent Ag mass basis. From stock solutions, experimental concentrations of $AgNO_3$ and AgNPs were prepared in EPA water ($NaHCO_3$ 0.096 g, $CaSO_4{\cdot}2H_2O$ 0.06 g, $MgSO_4{\cdot}7H_2O$ 0.06 g, KCl 0.004 g in DW 1 L). Particle shape and size of AgNPs were examined by Energy filtering transmission electron microscopy (TEM, LIBRA 120 TEM; Carl Zeiss) and particle size distribution in solution was determined by measuring hydrodynamic diameter (HDD) using dynamic light scattering (DLS, DLS-7000; Otsuka Electronics Co., Inc.).

2.2. C. elegans culture

C. elegans were grown in Petri dishes on nematode growth medium (NGM) and fed OP50 strain *Escherichia coli* according to a standard protocol (Brenner, 1974), with young adults (3 days) from an age-synchronized culture used in all the experiments. To produce age-synchronized cultures, at 2–3 days, eggs from mature adults were isolated using a 10% hypochlorite solution, followed by rinsing with S-buffer (129 mL 0.05 M K_2HPO_4, 871 mL 0.05 M KH_2PO_4, 5.85 g NaCl). The eggs were then allowed to hatch on agar plates with the OP50 food source, resulting in synchronized adult worm populations. *Wildtype* and mutants were provided by the Caenorhabditis Genetics Center at the University of Minnesota. A list of the mutant strains employed is presented in Supplementary Table 1.

2.3. Lethality test and estimation of LC_{50}

Lethality tests were performed on the *wildtype* after 24 h of exposure to different concentrations of $AgNO_3$ and AgNPs, as described previously (Roh et al., 2006). Briefly, each test consisted of four concentrations and a control, in which 20 ± 1 young *C. elegans* adults were transferred to 24 well tissue culture plates containing 1 mL of the test solution in each of five wells. The worms were exposed for 24 h at 20 °C. After 24 h, the numbers of live and dead worms were determined via visual inspection by probing with a platinum wire under a dissecting microscope. LC_{50} were derived through a Probits analysis.

2.4. Pharmaceutical rescue assay

To investigate the role of oxidative stress in AgNP induced toxicity, *C. elegans* were pretreated with 10 mg/L of N-acetyl cysteine (NAC) and trolox for 2 h followed by simultaneous treatment of 0.025, 0.05, 0.075 μg/mL, which corresponding about LC_{10}, LC_{50} and LC_{90} values, respectively, of $AgNO_3$ and bare AgNPs. After 24 h exposure, the worms were checked for survival.

2.5. ROS formation assay

To detect the levels of reactive oxygen species (ROS), *C. elegans* were exposed to AgNPs and $AgNO_3$ at LC_{10} and LC_{50} for 24 h, then transferred to 0.5 mL of S buffer, containing 50 μM 2, 7-dichlorofluoroscein diacetate (DCFH-DA, Sigma), a well-established compound to detect and quantify ROS (Eruslanov and Kusmartsev, 2010). The fluorescence was observed using a Leica DM IL microscope, with images obtained using a Leica DCF 420C camera (Leica). Levamisole (4 mM, Sigma–Aldrich) was applied to *C. elegans*, pictures of the live worms were then taken. Image analyses were conducted on five individual biological replications. To further quantify the ROS formation, *C. elegans* exposed to AgNPs and $AgNO_3$ at LC_{50} for 24 h were treated with DCFH-DA and the fluorescence was measured using COPAS™ (complex object parametric analysis and sorting) Select (Union Biometrica, Somerville, MA) with an excitation laser of 488 nm and emission wavelengths of 500–538 nm. A total of 600 worms were analyzed per condition.

2.6. Mitochondrial membrane potential measurement

Mitochondrial membrane potential ($\Delta\psi$m) was measured by using tetramethylrhodamine ethyl ester (TMRE, Sigma) staining. Age synchronized young adult were exposed to AgNPs and $AgNO_3$ at LC_{10} and LC_{50} for 24 h and 30 μM TMRE was added for staining, 3 h before harvest. Stained worms were imaged using a fluorescent microscope (DCF 420C, Leica), with excitation and emission wavelengths of between 570–610 nm. Carbonyl cyanide 3-chlorophenylhydrazone (CCCP) was used positive control. As with ROS formation, fluorescence from TMRE staining was also quantified using COPAS™ Select. The fluorescence was measured on TMRE stained *C.elegans* with an excitation laser of 543 nm and emission wavelengths of 575–640 nm. A total of 600 worms were analyzed per condition.

2.7. Oxidative DNA damage measurement

8-Hydroxydeoxyguanosine (8-OHdG) detection was carried out by Oxiselect™ Oxidative DNA damage ELISA Kit (Cell Biolabs, Inc.). The whole process was divided into major three steps- DNA extraction, DNA digestion and finally 8-OHdG detection. Age synchronized *C. elegans* strains were exposed at LC_{10} and LC_{50} of $AgNO_3$ and AgNPs for 24 h and preserved at −80 °C after washings in S buffer. DNA was extracted from homogenized *C. elegans* samples by using DNA extraction kit (DNeasy blood & Tissue kit, QIAGEN) and the quality and quantities were ascertained by spectrophotometer (EVO 60, ThermoScientific). The extracted DNA samples were converted to single stranded DNA by incubating at 95 °C for 5 min followed by rapid chilling on ice. Thereafter, 10 μL of nuclease P1 (Sigma–Aldrich; 0.5 U/μL dissolved in 20 mM sodium acetate, pH 5.3) was added to 100 μL of DNA (0.2–0.5 μg/μL). The samples were incubated at 37 °C for 2 h to hydrolyze DNA. Next, 10 μL of alkaline phosphatase (Biolabs; 0.5 U/μL dissolved in supplied NEBuffer-3, pH-7.9) were added to each sample and incubated for further 1 h at 37 °C. To remove all macromolecules and enzymes the hydrolysates were filtered (Microcone, Millipore) and centrifuged at 12 000 rpm for 5 min and the supernatant was used for 8OHdG ELISA assay. 8OHdG ELISA was performed by following supplier instructions. Briefly, the supplied ELISA plate was coated with 8-OHdG-conjugate (100 μL of 1 μg/mL to each well) and incubated overnight at 4 °C. On experiment day the coated wells were washed with 200 μL of assay diluents and blocked with the assay diluent at room temperature for 1 h. 50 μL of unknown samples and supplied 8-OHdG standards (ranging from 0 to 20 ng/mL) were added to the corresponding coated wells and incubated for 10 min at room temperature on an orbital shaker. After that, 50 μL of anti-8-OHdG antibody was added to each well and incubated for 1 h at room temperature with gentle shaking. After thorough washing with 1× wash buffer, 100 μL of secondary antibody-enzyme conjugate were added and incubated for 1 h. Then 100 μL of substrate were added to each well after another washing and incubated for 2–30 min until color formation. As soon as color was formed 100 μL of stop solution was added and the absorbance was measured at 450 nm in a 96-well ELISA plate reader (Sunrise-Basic-TECAN, Austria). The experiment performed with three different samples each with duplicate.

2.8. QPCR assay for detection of DNA lesions

Polymerase-blocking DNA damage was detected using a quantitative long amplicon PCR (QPCR) assay (Hunter et al., 2010; Meyer, 2010). Age synchronized *wildtype* and *cep-1(gk138)* young adults were exposed to $AgNO_3$ and AgNPs at LC_{10} for 24 h in 96-well plates, with 50 worms/well dispensed with a COPAS Biosort (Union Biometrica, Holliston MA). 50 J/m^2 ultraviolet C radiation (UVC) was used as a positive control for nuclear and mitochondria DNA damage. After 24 h of exposure, worms were transferred to no peptone plates to dry and half of the control nematodes were exposed to UVC as previously described (Bess et al., 2012). For each exposure condition, 6 nematodes were picked into 90 μL of the lysis buffer in triplicate, lysed, and analyzed for DNA damage. The exposures were carried out twice and all samples were analyzed by duplicate QPCR runs.

The QPCR assay detects any alterations to the genomic DNA template that result in altered PCR amplification of a large (~10 kb) region of the mitochondrial and nuclear genomes, such that damage of any sort ("lesions") results in reduced PCR product. The amplification of these large targets is normalized to genome copy number via measurement of mitochondrial and nuclear genomes using the amplification by real-time PCR of small mitochondrial and nuclear targets (Bess et al., 2012), in conjunction with standard curves (Hunter et al., 2010). Any reduction in PCR product, compared to control samples, is converted mathematically to a number of lesions per 10 kb (Hunter et al., 2010).

2.9. Statistics

Data are presented in arbitrary units compared to the control, with statistical differences between the *wildtype* and mutants relating to survival determined by an analysis of variance test, with a Tukey's post hoc test. All statistical tests were performed using Statistical Package for Social Sciences 12.0 (SPSS).

3. Results and discussion

3.1. Physicochemical properties

To determine the physicochemical properties of AgNPs, particle size distribution and shape were examined by DLS and TEM. The HDD of the AgNPs was between 35 and 108 nm using DLS measurements. The bare AgNPs appeared to be less aggregated than the coated nanoparticles. A comparison of two PVP AgNPs with different sizes (8 and 38 nm) showed that larger sized AgNPs (PVP38-AgNPs) tend to be more aggregated than their smaller counterparts (Fig. 1). TEM revealed round shaped aggregated particles but no particular trend was observed according to the coating and sizes (Fig. 1). Detailed physicochemical data for the PVP-coated AgNPs have been previously reported (Yang et al., 2012).

3.2. Comparative toxicity of $AgNO_3$, bare and PVP coated AgNPs

The 24 h-LC_{50}s of $AgNO_3$, bare AgNPs, PVP8-AgNPs and PVP38-AgNPs were estimated based on a *C. elegans* lethality test (Table 1). The LC_{50} of $AgNO_3$ and bare AgNPs was 0.05 mg/L, whereas it was 3 mg/L for PVP38-AgNPs. The order of toxicity was found to be $AgNO_3$ = bare AgNPs ≫ PVP8-AgNPs > PVP38-AgNPs. Thus, smaller PVP-AgNPs were more toxic than the larger nanoparticles. Our recent study on the AgNPs-induced hypoxia signaling pathway compared the AgNPs and Ag ion toxicities and found that AgNPs and $AgNO_3$ did not show any qualitative difference in terms of toxicity in the observed pathways. On the other hand, the AgNPs were generally more toxic than an equal amount of silver in $AgNO_3$ (Eom et al., 2013). The results of another comparative study of AgNPs and Ag ions using *Daphnia magna* and *Pimephales promelas* are also consistent with the present study because they did not provide strong evidence that AgNPs either acts via a different mechanism of toxicity than Ag ions or is likely to cause acute or lethal toxicity beyond which would be predicted by the mass concentration of silver (Hoheisel et al., 2012). In the present study, the PVP8-AgNPs had higher toxicity than PVP38-AgNPs, however, in our previous

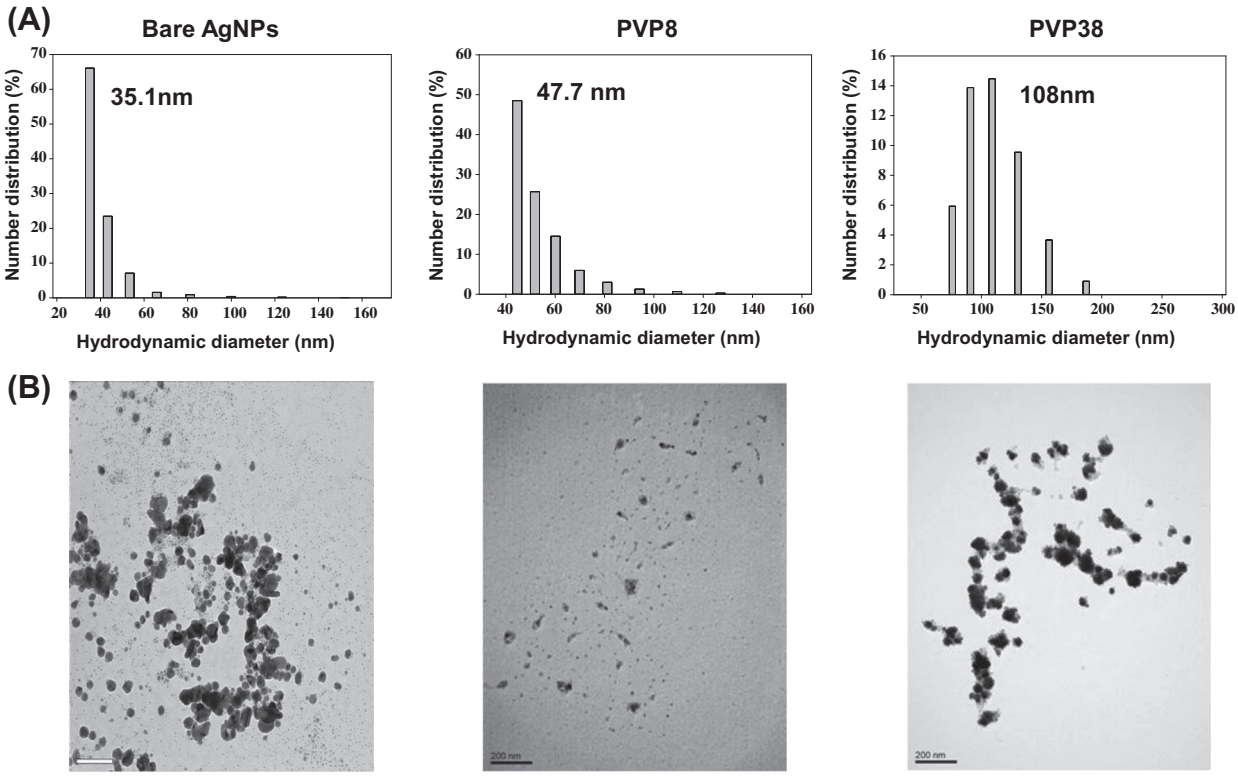

Fig. 1. Characterization of silver nanoparticle. Particle shapes and the size distribution were analyzed by TEM (A) and DLS (B).

Table 1
Estimation of LC_{50} after exposure to $AgNO_3$, AgNPs, PVP8 and PVP38 in *wildtype C. elegans*.

EPA water	24 h LC (mg/L)	Interval of confidence (95%)
$AgNO_3$		
LC_{10}	0.029	0.016 < LC 10 < 0.037
LC_{50}	**0.046**	0.037 < LC 50 < 0.054
LC_{90}	0.074	0.062 < LC 90 < 0.107
Bare AgNPs		
LC_{10}	0.026	0.017 < LC 10 < 0.032
LC_{50}	**0.041**	0.034 < LC 50 < 0.048
LC_{90}	0.066	0.055 < LC 90 < 0.090
PVP8-AgNPs		
LC_{10}	0.409	0.259 < LC 10 < 0.494
LC_{50}	**0.607**	0.507 < LC 50 < 0.687
LC_{90}	0.901	0.782 < LC 90 < 1.212
PVP38-AgNPs		
LC_{10}	1.625	0.737 < LC 10 < 2.227
LC_{50}	**3.262**	2.466 < LC 50 < 4.026
LC_{90}	6.547	5.067 < LC 90 < 11.852

study, we found the opposite trend with these two particles using a *C. elegans* growth inhibition assay (Yang et al., 2012). Different endpoints (mortality vs. growth inhibition) applied for the comparison may be one of the reasons of this discrepancy. In another AgNPs toxicity study using 12 and 21 nm sized particles, the 12 nm particles were found to be more bioactive with a LC_{50} of 15.8 μg/mL compared to 50.1 μg/mL for the 21 nm sized particles on zebra fish embryos (Cowart et al. 2011). Therefore, although size dependent toxicity is frequently observed in nanotoxicity (Oberdörster et al., 2005; Pan et al., 2007; Park et al., 2011; Kim et al., 2012) other physicochemical parameters of the particle, as well as experimental factors (i.e. endpoints, exposure conditions, test media) also affect bioavailability and toxicity (Hussain et al., 2005; Eom and Choi, 2010; Choi et al., 2014).

3.3. Stress response mutant screening

In our previous study on comparative toxicity, no mechanistic difference was observed between $AgNO_3$ and bare AgNPs (Eom et al., 2013), whereas in another previous study, we found distinct mechanisms were involved in toxicity of PVP8- and PVP38-AgNPs (Yang et al., 2012). In this study, after confirming the different toxic potential of $AgNO_3$ and AgNPs, we examined whether distinct and/or common toxic mechanisms are related to the differential sensitivity. To answer this question, various stress response mutants of *C. elegans* were exposed to $AgNO_3$ and AgNPs, and the response of each mutant to different types of silvers was compared with that of the *wildtype*. As the response of each mutant to silver might indicate the underlying mechanism, a comparison of the response of different stress response mutants to that of *wildtype* is an efficient way of gaining insight into the mechanism of chemical toxicity (Roh et al., 2009). A broad range of stress response mutants including strains deficient in responses to general stress (*hsp-16.2(gk249)*, *daf-16(mu86)*, *daf-2(e1370)*, *sgk-1(ok538)*, *akt-1(ok525)* and *akt-2(ok393)*); immune response (*pmk-1(km25)*); metal stress (*mtl-2(gk125)*); oxidative stress (*sod-1(tm776)*, *sod-3(gk235)* and *ctl-2(ok1996)*); DNA damage and oxidative stress (*cep-1(gk138)*, *ced-3(n717)* and *ced-4(n1162)*); and metabolic stress indicators (*ire-1(ok799)*, *sir-2.1(ok434)* and *aak-2(gt33)*) was used for screening (Fig. 2).

The mutants of the genes in metabolic stress (*aak-2(gt33)* and *sir-2.1(ok434)*), apoptosis (*ced-3(n717)*) and immune response (*pmk-1(km25)*) were the mutants most sensitive to bare AgNPs exposure (with survival rates reduced to 50–90% of controls), whereas, *pmk-1* and the mutants of the genes in the *daf-16* pathway (*akt-1(ok525)* and *sgk-1(ok538)*) were found to be most sensitive to $AgNO_3$ exposure. Regarding the PVP-coated AgNPs, no significant difference was observed in any of mutants tested compared to the *wildtype*. The mutants screening test generally

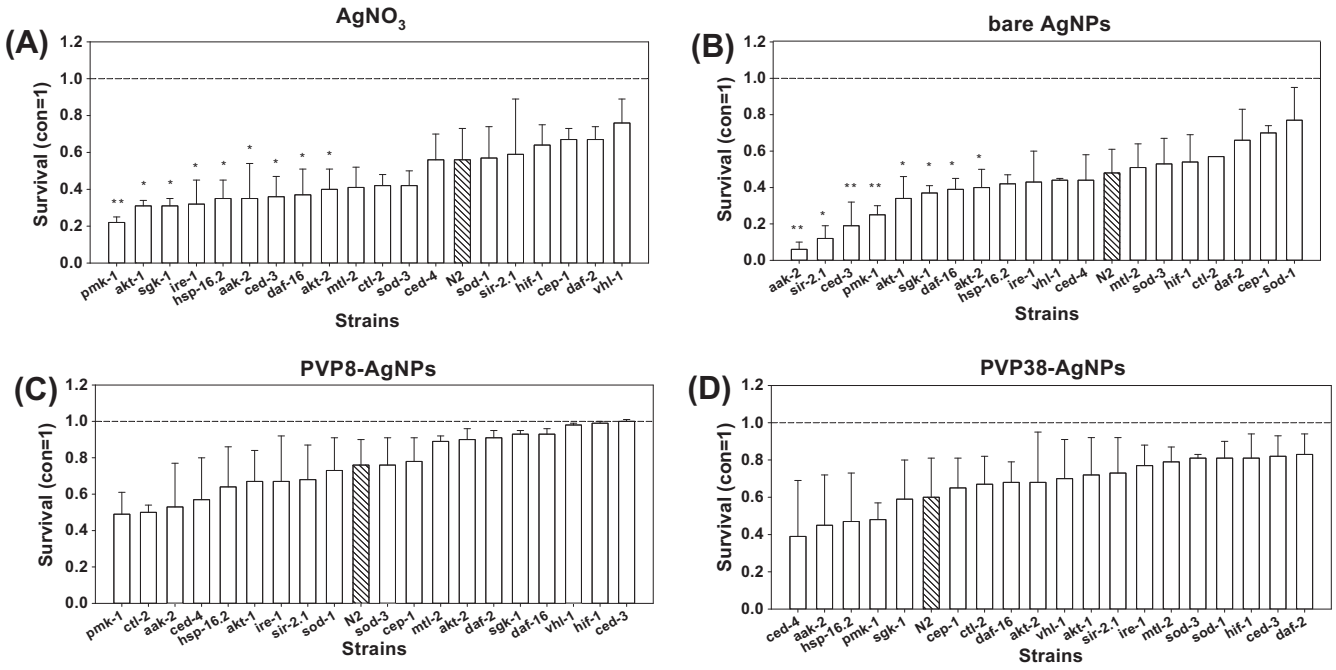

Fig. 2. Survival of *C. elegans* strains *wildtype* and mutants. Survival test was conducted on *wildtype(N2)* and mutants *C. elegans* exposed to $AgNO_3$ (A), bare AgNPs (B), PVP8 (C) and PVP38 (D) for 24 h. The results were expressed as the mean value compared to control (control = 1, $n = 3$; mean ± standard error of the mean; $^{*}p < 0.01$, $^{**}p < 0.005$).

suggests that $AgNO_3$ and AgNPs may cause toxicity via a different mechanism, but no clear similar or distinct response was found. Moreover, the mutant strains' response was not sensitive enough to permit detection of the toxicity of the PVP-coated AgNPs, despite the fact that LC_{50} concentrations were used. This suggests that either the mechanism of toxicity of the PVP-coated AgNPs is general, or pathways different than those tested are important. A range of stress response mechanisms, such as, metabolic stress, apoptosis and immune response appears to be involved in the toxicity of bare AgNPs (Fig. 2).

In the current study, *pmk-1(km25)*, *ced-3(n717)* and *ced-4(n1162)* were generally the most sensitive mutants. Moreover, previous studies have suggested that oxidative stress is involved in the AgNPs toxicity in *C. elegans* (Roh et al., 2009; Lim et al., 2012; Yang et al., 2012; Eom et al., 2013). In particular, *pmk-1* dependant oxidative stress in AgNPs-exposed *C. elegans* has been studied extensively (Lim et al., 2012; Eom et al., 2013). Therefore, in the next step, this study examined whether $AgNO_3$ or AgNPs would cause oxidative stress focusing on mitochondrial and DNA damage.

3.4. Oxidative stress

In many systems, dissolved Ag ions released from the surface of the AgNPs make a significant contribution to AgNPs toxicity. Our previous study compared the rescue of toxicity by the antioxidant agent, NAC, which acts as a ROS scavenger and Ag ion chelator, with rescue by another antioxidant, trolox, which only acts as a ROS scavenger (Yang et al., 2012). The present study examined whether the toxicity of bare AgNPs is dependent on the dissolved Ag ions or intrinsic toxicity (oxidative stress) by comparing the rescue effect of NAC and trolox with that of $AgNO_3$ (Fig. 3). As expected, the toxicity of the AgNPs was rescued by both antioxidant pharmaceuticals, whereas that of $AgNO_3$ was rescued only by NAC but not by trolox. The fact that the toxicity of $AgNO_3$ was not rescued by trolox, whereas that of AgNPs was mostly rescued by trolox, suggests that the toxicity of bare AgNPs is largely due to ROS and only partially due to dissolved Ag ions.

Oxidative stress was directly investigated by measuring ROS formation in *C. elegans* exposed to $AgNO_3$ and AgNPs after DCFH-DA staining using the fluorescence microscopy and the COPAS™ Select (Fig. 4). Though a statistical difference was not found between bare AgNPs and $AgNO_3$ (Fig. 4B), ROS formation seems to be more important in the bare AgNPs exposed worms than in the $AgNO_3$ exposed ones (Fig. 4A and B), which supports the rescue toxicity results with pharmaceuticals (Fig. 3). Among coated-AgNPs, we expected higher florescence signal in PVP38-AgNPs exposed worms than PVP8-AgNPs exposed ones, as we previously reported that the toxicity of PVP38-AgNPs was due to ROS generation, whereas the toxicity of PVP8-AgNPs was due to dissolved Ag ions by using pharmaceutical and genetic experiments. However, in this study, we found no clear difference in fluorescence signal in PVP-coated AgNPs exposed worms at both concentrations tested, which may be due to lower sensitivity of this imaging experiment than the previously applied pharmaceutical or genetic approaches.

3.5. Mitochondrial damage

In the next step, we investigated whether $AgNO_3$ and AgNPs affect mitochondria by measuring mitochondrial membrane potential ($\Delta\psi m$) with TMRE staining using the fluorescence microscopy and the COPAS™ Select (Fig. 5). Decreased membrane potential was identified by decreased fluorescence after TMRE staining in CCCP (a positive control) exposed worms. At the lower concentration (LC_{10}), no change was found in any of exposed worms compared to control, however at the concentration of LC_{50}, the decreased fluorescence was observed in *C. elegans* exposed to $AgNO_3$, bare and PVP8-AgNPs (Fig. 5A), which was also observed with quantification result measured using COPAS™ Select (Fig. 5B). The result therefore suggests that AgNPs possesses the potential to alter mitochondrial membrane permeability in *C. elegans*. Other studies also suggest mitochondria are a main subcellular target organelles of AgNPs (AshaRani et al. 2009; Teodoro et al. 2011). Observation of the AgNPs inside the mitochondria and nucleus by TEM led to the proposal that disruption of the mito-

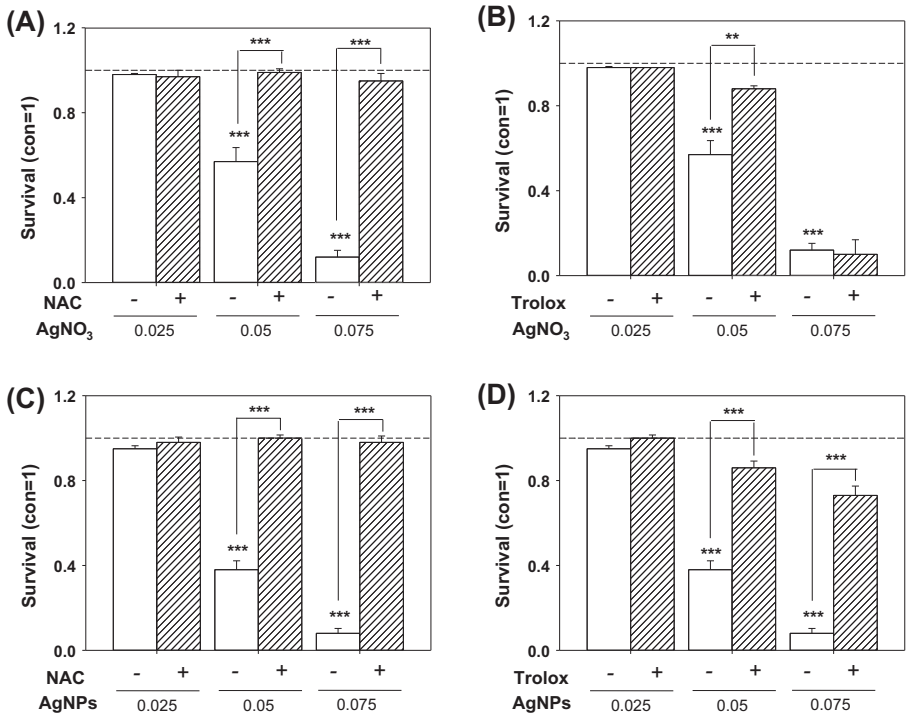

Fig. 3. Rescue assay with N-acetyl cysteine (NAC) and trolox. Survival analysis was conducted on *wildtype(N2) C. elegans* exposed to $AgNO_3$ (A and B), bare AgNPs (C and D). The results are expressed as the mean value compared to control (control = 1, $n = 3$; mean ± standard error of the mean; $^{***}p < 0.001$). The statistical difference on NAC and trolox treatment was also analyzed ($^{**}p < 0.005$, $^{***}p < 0.001$).

chondrial respiratory chain by the AgNPs leading to the production of ROS and interruption of ATP synthesis, in turn causing DNA damage, was a possible mechanism for the toxicity of AgNPs to cells. It was also reported that AgNPs induced alterations of mitochondrial membrane permeability and uncoupling of the oxidative phosphorylation system in cells. These *in vitro* studies suggest mitochondrial toxicity may play a central role in the toxicity resulting from exposure to AgNPs and this study supports this idea in an *in vivo* model.

3.6. DNA damage

The final step of this study was to determine if $AgNO_3$ and AgNPs would induce DNA damage using two complementary methods, detection of oxidative base modification and polymerase-inhibiting lesions. The guanine base modification 8-OHdG was measured as a marker of oxidative DNA damage (Fig. 6), and DNA polymerase-inhibiting DNA lesions were measured by QPCR, which is capable of detecting a wider range of DNA damage, including strand breaks, adducts, dimers, crosslinks, etc. (Meyer, 2010) (Fig. 7). The mitochondrial genome is believed more sensitive to many genotoxic chemicals than the nuclear genome (Meyer, 2010; Meyer et al., 2013), and the present results also suggested AgNPs possess potential to increase mitochondrial membrane permeability in nematodes (Fig. 5). Therefore, the QPCR assay was conducted separately on the mitochondria and nuclear genomes.

The oxidative DNA damage assay revealed a significant increase in 8-OHdG levels in $AgNO_3$- and bare AgNPs-exposed *C. elegans*, with the greatest significance resulting from exposure to bare AgNPs at both concentrations tested. On the other hand, PVP8-AgNPs induced an increase in the 8-OHdG levels only at the concentration of LC_{50}, and much more moderately than $AgNO_3$ and bare AgNPs. No increase was observed after PVP38-AgNPs exposure (Fig. 6). By QPCR, the level of nuclear DNA (nDNA) damage observed after exposing the nematodes to UVC was significantly higher than the controls ($p < 0.0001$), but neither $AgNO_3$ nor any of the AgNPs tested resulted in increased damage compared to the controls ($p > 0.05$ in all cases) (Fig. 7A). Mitochondrial DNA (mtDNA) damage was also observed after exposure to UVC. Again, the UVC-exposed nematodes had significantly more mtDNA damage than the controls ($p < 0.0001$), but no other treatments resulted in increased damage compared to the controls ($p > 0.05$ in all cases) (Fig. 7B). The mtDNA:nDNA ratio was also investigated but no significant trend was observed in any of the samples tested (Fig. 7C). Because we obtained negative results with *wildtype C. elegans*, we additionally conducted the same experiments using a DNA damage sensitive strain, *cep-1(gk138)*, which lacks the *C. elegans* homolog of p53. However, none of the types of silver tested led to an increase in DNA lesions either in nDNA or mtDNA of the *cep-1(gk138)* strain.

The apparently contradictory result of lack of detection of DNA damage with QPCR, but positive results with the 8-OHdG assay may result from a number of factors. First, the QPCR has a higher limit of detection (~1 lesion/100 000 bases; Meyer, 2010) than the ELISA 8-OHdG assay (100 pg/mL 8-OHdG). Another factor could be the fact that the damage caused by these exposures is primarily small oxidative modification of bases including 8-OHdG, which may be hard to detect via QPCR (Meyer, 2010). Genotoxicity of AgNPs has been conducted mostly in *in vitro* models and only limited *in vivo* studies are available so far. In a study using Sprague–Dawley rat, negative results were obtained using the micronucleus test (Kim et al., 2008), whereas, positive results were observed in another *in vivo* study with *Drosophila* by using the wing somatic mutation and recombination test (Demir et al., 2011). In this sense, the current investigation on *C. elegans* adds new information on the *in vivo* genotoxic effects of AgNPs.

We found a strong increase in oxidative DNA damage in both bare AgNPs- and $AgNO_3$-exposed *C. elegans* (Fig. 6). However, most other AgNPs genotoxicity studies reported that AgNPs have higher genotoxic potential than Ag ions. When apoptosis and oxidative

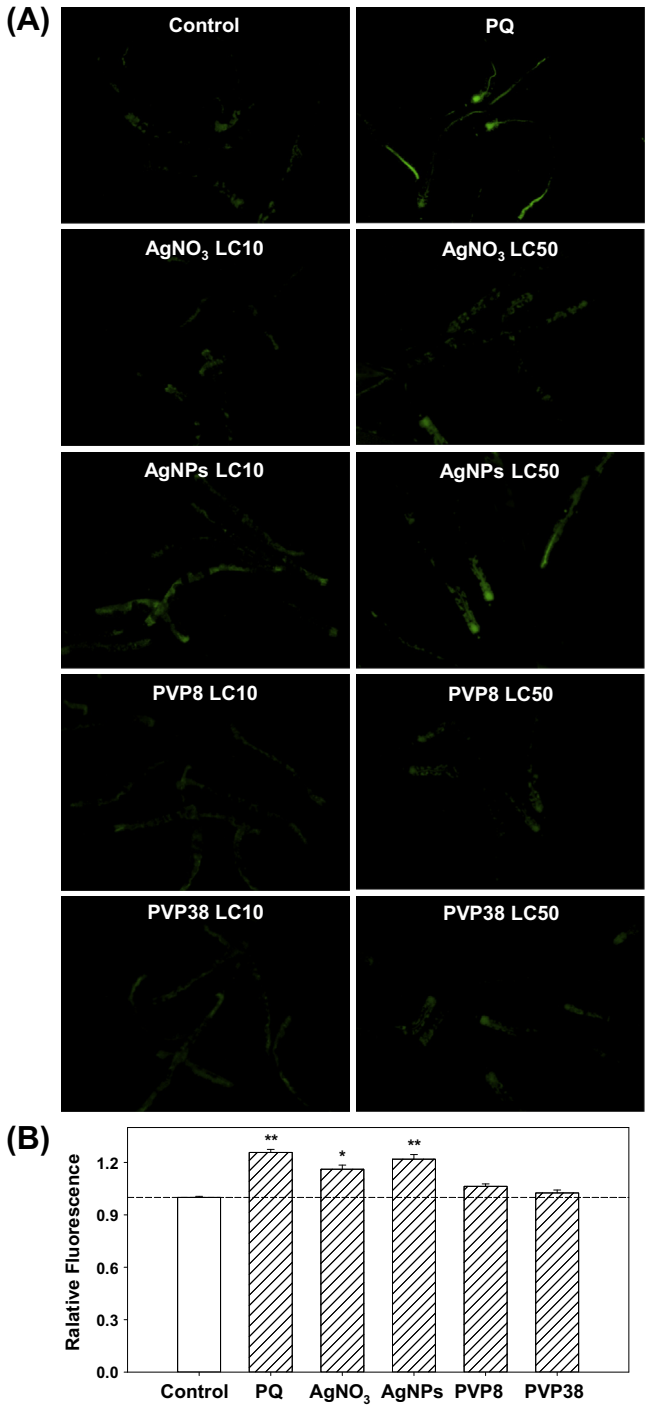

Fig. 4. The formation of reactive oxygen species (ROS). The level of ROS were measured in *wildtype(N2) C. elegans* exposed to $AgNO_3$, bare AgNPs, PVP8 and PVP38 at LC_{10} and LC_{50} for 24 h using fluorescence microscopy (A). The fluorescence intensity was quantified in *wildtype(N2) C. elegans* exposed to $AgNO_3$, bare AgNPs, PVP8 and PVP38 at LC_{50} for 24 h using COPAS Select ($\geqslant$600 worms per conditions) (B). Worms were incubated 50 μM 2,7-dichlorofluoroscein diacetate (DCFH-DA) at 20 °C for 30 min and paraquat was used as a positive control. The result of fluorescence intensity was expressed as the mean value compared to control (control = 1; mean standard error of the mean; $^{*}p < 0.01$, $^{**}p < 0.005$).

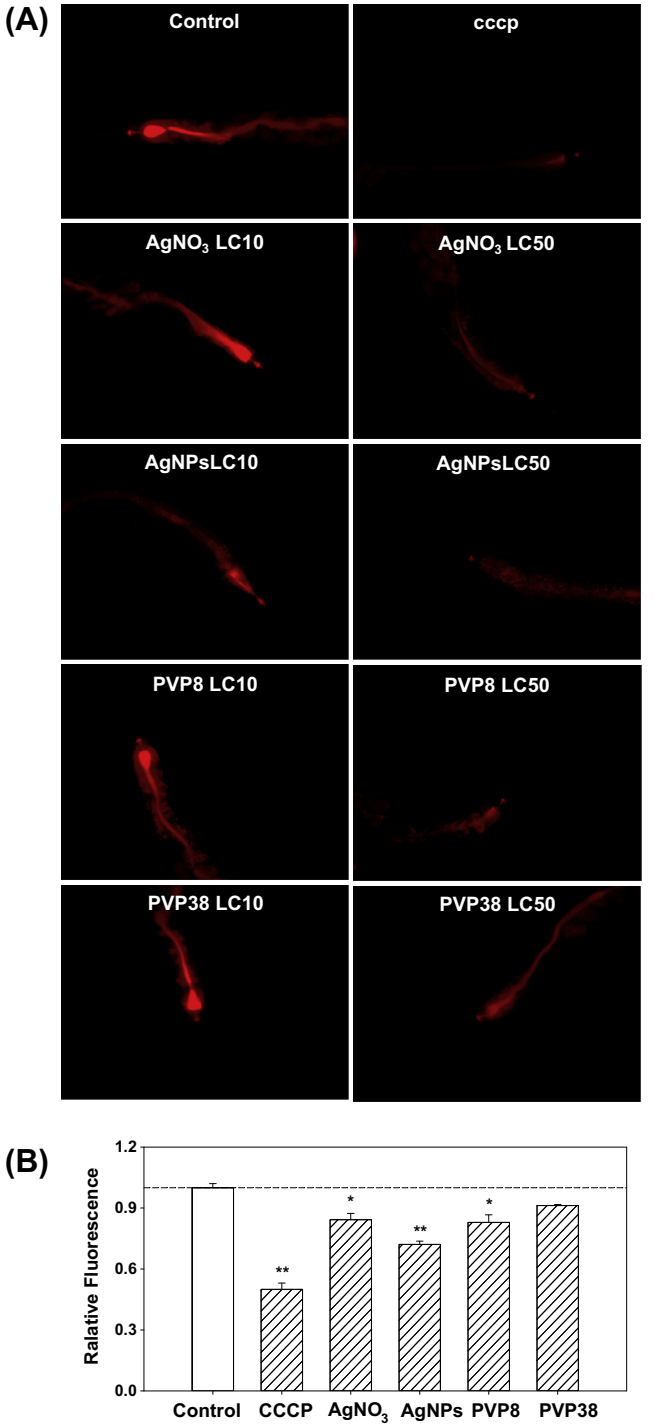

Fig. 5. Analysis of mitochondrial membrane potential ($\Delta\psi$m). Mitochondrial potential permeability was measured in *wildtype(N2) C. elegans* exposed to $AgNO_3$, bare AgNPs, PVP8 and PVP38 at LC_{10} and LC_{50} for 24 h using fluorescence microscopy (A). The fluorescence intensity was quantified in *wildtype(N2) C. elegans* exposed to $AgNO_3$, bare AgNPs, PVP8 and PVP38 at LC_{50} for 24 h using COPAS Select ($\geqslant$600 worms per conditions) (B). Worms were incubated tetramethylrhodamine ethyl ester (TMRE) at 20 °C for 3 h and carbonyl cyanide 3-chloro phenyl hydrazine (CCCP) was used as a positive control. The result of fluorescence intensity was expressed as the mean value compared to control (control = 1; mean standard error of the mean; $^{*}p < 0.01$, $^{**}p < 0.005$).

stress were evaluated in HeLa cells (Miura and Shinohara, 2009) and when the frequency of micronucleus formation was measured in HepG2 cells (Kawata et al., 2009), AgNPs caused much stronger damage than Ag ions. In above mentioned *Drosophila* study, genotoxicity via somatic recombination was observed only with AgNPs but not with $AgNO_3$ (Demir et al., 2011). It was also found in a study with Japanese medaka that AgNPs caused DNA damage as well as oxidative and carcinogenic stress, while Ag ion only in-

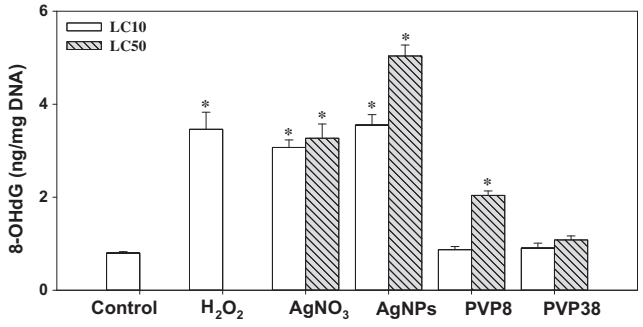

Fig. 6. Measurement of 8-OHdG levels. Levels of 8-OHdG were measured in *wildtype(N2) C. elegans* exposed to $AgNO_3$, bare AgNPs, PVP8 and PVP38 by ELISA kit. The results were expressed as the mean value ($n = 3$, mean ± standard error of the mean; $^*p < 0.01$).

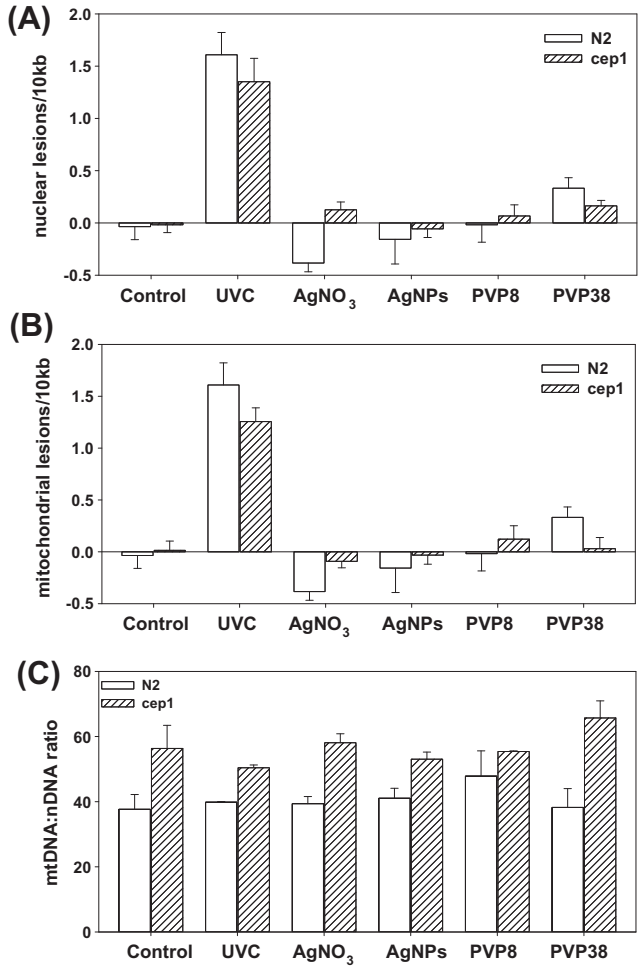

Fig. 7. QPCR assay of nuclear and mitochondrial DNA damage. Polymerase-inhibiting DNA lesions were measured in *wildtype* and *cep-1(gk138) C. elegans* exposed to $AgNO_3$ or AgNPs, using QPCR in the nuclear genome (A) and mitochondrial genome (B). The mitochondrial:nuclear DNA ratio was measured in the same nematodes (C). UVC was used as the positive control. The results were expressed as the mean value (mean ± standard error of the mean, $n = 3$).

duced inflammation, metallic detoxification response and low overall stress response (Chae et al., 2009). Here, we found both AgNPs and $AgNO_3$ led to an increase of 8-OHdG. The most significant increase was found in worms exposed to AgNPs at the LC_{50} (5-fold compared to control, Fig. 6), which supports previous studies that found more DNA damage after AgNPs exposure than after $AgNO_3$ exposure. The facts that toxicity of bare AgNPs was rescued by trolox, but that of $AgNO_3$ was not (Fig. 3), and that the formation of ROS was more important in bare AgNPs exposed worms than in $AgNO_3$ exposed ones (Fig. 4), also supports a mechanism of DNA damage resulting from generation of reactive oxygen species by AgNPs.

In this study, we found that PVP-coated AgNPs were less toxic than bare AgNPs and $AgNO_3$ in almost every endpoint tested (i.e. LC_{50} (Table 1), mutant sensitivity test (Fig. 2), ROS formation (Fig. 4), mitochondrial membrane permeability (Fig. 5), oxidative DNA damage (Fig. 6). Coatings may reduce ion release from AgNPs, thus toxicity from released Ag ions would be lower in PVP-AgNPs than in bare AgNPs. A higher agglomeration potential of PVP-AgNPs in the media than bare AgNPs was shown by the HDD measurement (Fig. 1); therefore, extensive agglomerations also may reduce the particle uptake and thus toxicity. In a genotoxicity study with PVP-AgNPs in Beas-2B cells, PVP-coated AgNPs were not able to induce chromosomal damage measured by micronucleus and chromosomal aberration assays, suggesting that PVP coating may protect cells from direct interaction with AgNPs (Nymark et al. 2013).

4. Conclusion

This comparative toxicity study showed that $AgNO_3$ and bare AgNPs exert a similar level of toxicity, whereas a PVP coating reduced the toxicity of AgNPs significantly. Size dependent toxicity was observed in the PVP-AgNPs. Different groups of mutants responded to $AgNO_3$ and AgNPs, suggesting distinct mechanisms of toxicity. None of the silver materials tested caused DNA lesions detectable by QPCR, but $AgNO_3$, bare AgNPs and PVP8-AgNPs did induce some oxidative DNA damage. $AgNO_3$ and AgNPs also affect mitochondrial membrane permeability. Overall, the results show that coatings on the AgNPs surface and the particle size contribute to the toxicity of AgNPs, and oxidative stress-related mitochondrial and DNA damage appear to be a potential mechanism of toxicity. Although the relationships between the genotoxic responses and physiological effects are complicated because of the compensatory mechanisms that regulate the physiological fitness, genotoxicity is an important area of ecotoxicological research from both mechanistic and biomonitoring perspectives. Therefore, the genotoxic potential of $AgNO_3$ and bare and coated AgNPs reported here using an *in vivo* model will shed more light on the impact of AgNPs on human and environmental health and will also help understand the potential consequences of unintended exposure.

Acknowledgements

This work was supported by Mid-career Researcher Program through the National Research Foundation of Korea (NRF) funded by the Ministry of Science, ICT and Future Planning (2013R1A2A2A03010980) and by Korea Ministry of Environment as "The Environmental Health Action Program" (2012001370009). This work was also supported by the National Science Foundation (NSF) and the Environmental Protection Agency (EPA) under NSF Cooperative Agreement EF-0830093, Center for the Environmental Implications of NanoTechnology (CEINT). Any opinions, findings, conclusions or recommendations expressed in this material are those of the author(s) and do not necessarily reflect the views of the NSF or the EPA. This work has not been subjected to EPA review and no official endorsement should be inferred.

Appendix A. Supplementary material

Supplementary material associated with this article can be found, in the online version, at http://dx.doi.org/10.1016/j.chemosphere.2014.01.078.

Reference

Ahamed, M., Karns, M., Goodson, M., Rowe, J., Hussain, S.M., Schlager, J.J., Hong, Y., 2008. DNA damage response to different surface chemistry of silver nanoparticles in mammalian cells. Toxicol. Appl. Pharmacol. 233, 404–410.

Arora, S., Jain, J., Rajwade, J.M., Paknikar, K.M., 2008. Cellular responses induced by silver nanoparticles: in vitro studies. Toxicol. Lett. 179, 93–100.

Arora, S., Jain, J., Rajwade, J.M., Paknikar, K.M., 2009. Interactions of silver nanoparticles with primary mouse fibroblasts and liver cells. Toxicol. Appl. Pharmacol. 236, 310–318.

Asare, N., Instanes, C., Sandberg, W.J., Refsnes, M., Schwarze, P., Kruszewski, M., Brunborg, G., 2012. Cytotoxic and genotoxic effects of silver nanoparticles in testicular cells. Toxicology 291, 65–72.

AshaRani, P.V., Low Kah Mun, G., Hande, M.P., Valiyaveettil, S., 2009. Cytotoxicity and genotoxicity of silver nanoparticles in human cells. ACS Nano 3, 279–290.

Bess, A.S., Crocker, T.L., Ryde, I.T., Meyer, J.N., 2012. Mitochondrial dynamics and autophagy aid in removal of persistent mitochondrial DNA damage in *Caenorhabditis elegans*. Nucleic Acids Res. 2012 (40), 7916–7931.

Brenner, S., 1974. The genetics of *Caenorhabditis elegans*. Genetics 77, 71–94.

Chae, Y.J., Pham, C.H., Lee, J., Bae, E., Yi, J., Gu, M.B., 2009. Evaluation of the toxic impact of silver nanoparticles on Japanese medaka (*Oryzias latipes*). Aquat. Toxicol. 94, 320–327.

Chatterjee, N., Eom, H.J., Choi, J., 2014. Silver nanoparticle induced oxidative DNA damage-repair as a function of p38MAPK status: a comparative approach using Jurkat T cells and the nematode *Caenorhabditis elegans*. Environ. Mol. Mutagen. 55, 122–133.

Choi, J., Tsyusko, O.V., Unrine, J.M., Chattergee, N., Ahn, J.M., Yang, X., Thornton, B.L., Ryde, I.T., Starnes, D., Meyer, J.N., 2014. A micro-sized model for the in vivo studies of nanoparticle toxicity: what has *Caenorhabditis elegans* taught us? Environ. Chem. (in press).

Cong, Y., Banta, G.T., Selck, H., Berhanu, D., Valsami-Jones, E., Forbes, V.E., 2011. Toxic effects and bioaccumulation of nano-, micron- and ionic-Ag in the polychaete, Nereis diversicolor. Aquat. Toxicol. 105, 403–411.

Cowart, D.A., Guida, S.M., Shah, S.I., Marsh, A.G., 2011. Effects of Ag nanoparticles on survival and oxygen consumption of zebra fish embryos, Danio rerio. J. Environ. Sci. Health A Toxicol. Hazard. Subst. Environ. Eng. 46, 1122–1128.

Croes, S., Stobberingh, E.E., Stevens, K.N.J., Knetsch, M.L.W., Koole, L.H., 2012. Antimicrobial and anti-thrombogenic features combined in hydrophilic surface coatings for skin-penetrating catheters. Synergy of co-embedded silver particles and heparin. Appl. Mater. Interf. 8, 2543–2550.

Demir, E., Vales, G., Kaya, B., Creus, A., Marcos, R., 2011. Genotoxic analysis of silver nanoparticles in Drosophila. Nanotoxicology 5, 417–424.

Eom, H.J., Choi, J., 2010. P38 MAPK activation, DNA damage, cell cycle arrest and apoptosis as mechanisms of toxicity of silver nanoparticles in Jurkat T cells. Environ. Sci. Technol. 44, 8337–8342.

Eom, H.J., Ahn, J.M., Kim, Y., Choi, J., 2013. Hypoxia inducible factor-1 (HIF-1)-flavin containing monooxygenase-2 (FMO-2) signaling acts in silver nanoparticles and silver ion toxicity in the nematode *Caenorhabditis elegans*. Toxicol. Appl. Pharmacol. 270, 106–113.

Eruslanov, E., Kusmartsev, S., 2010. Identification of ROS using oxidized DCFDA and flow-cytometry. Methods Mol. Biol. 594, 57–72.

Foldbjerg, R., Dang, D.A., Autrup, H., 2011. Cytotoxicity and genotoxicity of silver nanoparticles in the human lung cancer cell line, A549. Arch. Toxicol. 85, 743–750.

Fubini, B., Ghiazza, M., Fenoglio, I., 2010. Physico-chemical features of engineered nanoparticles relevant to their toxicity. Nanotoxicology 4, 347–363.

Gopinath, P., Gogoi, S.K., Sanpui, P., Paul, A., Chattopadhyay, A., Ghosh, S.S., 2010. Signaling gene cascade in silver nanoparticle induced apoptosis. Colloids Surf., B 77, 240–245.

Hackenberg, S., Scherzed, A., Kessler, M., Hummel, S., Technau, A., Froelich, K., Ginzkey, C., Koehler, C., Hagen, R., Kleinsasser, N., 2011. Silver nanoparticles: evaluation of DNA damage, toxicity and functional impairment in human mesenchymal stem cells. Toxicol. Lett. 201, 27–33.

Hoheisel, S.M., Diamond, S., Mount, D., 2012. Comparison of nanosilver and ionic silver toxicity in *Daphnia magna* and *Pimephales promelas*. Environ. Toxicol. Chem. 31, 2557–2563.

Hsin, Y.H., Chen, C.F., Huang, S., Shih, T.S., Lai, P.S., Chueh, P.J., 2008. The apoptotic effect of nanosilver is mediated by a ROS and JNK-dependent mechanism involving the mitochondrial pathway in NIH3T3 cells. Toxicol. Lett. 179, 130–139.

Hunter, S.E., Jung, D., Di Giulio, R.T., Meyer, J.N., 2010. The QPCR assay for analysis of mitochondrial DNA damage, repair, and relative copy number. Methods 51, 444–451.

Hussain, S.M., Hess, K.L., Gearhart, J.M., Geiss, K.T., Schlager, J.J., 2005. In vitro toxicity of nanoparticles in BRL 3A rat liver cells. Toxicol. In Vitro 19, 975–983.

Ivask, A., Elbadawy, A., Kaweeteerawat, C., Boren, D., Fischer, H., Ji, Z., Chang, C.H., Liu, R., Tolaymat, T., Telesca, D., Zink, J.I., Cohen, Y., Holden, P.A., Godwin, H.A., 2014. Toxicity mechanisms in *Escherichia coli* vary for silver nanoparticles and differ from ionic silver. ACS Nano. 8, 374–386.

Jiang, J., Oberdörster, G., Biswas, P., 2009. Characterization of size, surface charge, and agglomeration state of nanoparticle dispersions for toxicological studies. J. Nanopart. Res. 11, 77–89.

Kawata, K., Osawa, M., Okabe, S., 2009. In vitro toxicity of silver nanoparticles at noncytotoxic doses to HepG2 human hepatoma cells. Environ. Sci. Technol. 43, 6046–6051.

Kim, Y.S., Kim, J.S., Cho, H.S., Rha, D.S., Kim, J.M., Park, J.D., Choi, B.S., Lim, R., Chang, H.K., Chung, Y.H., Kwon, I.H., Jeong, J., Han, B.S., Yu, I.J., 2008. Twenty-eight-day oral toxicity, genotoxicity, and gender-related tissue distribution of silver nanoparticles in Sprague–Dawley rats. Inhal. Toxicol. 20, 575–583.

Kim, S., Choi, J.E., Choi, J., Chung, K.H., Park, K., Yi, J., Ryu, D.Y., 2009. Oxidative stress-dependent toxicity of silver nanoparticles in human hepatoma cells. Toxicol. In Vitro 23, 1076–1084.

Kim, T.H., Kim, M., Park, H.S., Shin, U.S., Gong, M.S., Kim, H.W., 2012. Size-dependent cellular toxicity of silver nanoparticles. J. Biomed. Mater. Res. A. 100, 1033–1043.

Lamb, J.G., Hathaway, L.B., Munger, M.A., Raucy, J.L., Franklin, M.R., 2010. Nanosilver particle effects on drug metabolism in vitro. Drug Metab. Dispos. 38, 2246–2251.

Leung, M.C.K., Williams, P.L., Benedetto, A., Au, C., Helmcke, K.J., Aschner, M., Meyer, J.N., 2008. *Caenorhabditis elegans*: an emerging model in biomedical and environmental toxicology. Toxicol. Sci. 10, 5–28.

Lim, D., Roh, J.Y., Eom, H.J., Choi, J.Y., Hyun, J., Choi, J., 2012. Oxidative stress-related PMK-1 P38 MAPK activation as a mechanism for toxicity of silver nanoparticles to reproduction in the nematode *Caenorhabditis elegans*. Environ. Toxicol. Chem. 31, 585–592.

Meyer, J.N., 2010. QPCR: a tool for analysis of mitochondrial and nuclear DNA damage in ecotoxicology. Ecotoxicology 19, 804–811.

Meyer, J.N., Leung, M.C., Rooney, J.P., Sendoel, A., Hengartner, M.O., Kisby, G.E., Bess, A.S., 2013. Mitochondria as a target of environmental toxicants. Toxicol. Sci. 134, 1–17.

Miura, N., Shinohara, Y., 2009. Cytotoxic effect and apoptosis induction by silver nanoparticles in HeLa cells. Biochem. Biophys. Res. Commun. 390, 733–737.

Mukherjee, S.G., O'Claonadh, N., Casey, A., Chambers, G., 2012. Comparative in vitro cytotoxicity study of silver nanoparticle on two mammalian cell lines. Toxicol. In Vitro 26, 238–251.

Navarro, E., Piccapietra, F., Wagner, B., Marconi, F., Kaegi, R., Odzak, N., Sigg, L., Behra, R., 2008. Toxicity of Silver Nanoparticles to Chlamydomonas reinhardtii. Environ. Sci. Technol. 42, 8959–8964.

Nymark, P., Catalán, J., Suhonen, S., Järventaus, H., Birkedal, R., Clausen, P.A., Jensen, K.A., Vippola, M., Savolainen, K., Norppa, H., 2013. Genotoxicity of polyvinylpyrrolidone-coated silver nanoparticles in BEAS 2B cells. Toxicol. 313, 38–48.

Oberdörster, G., Oberdörster, E., Oberdörster, J., 2005. Nanotoxicology: an emerging discipline evolving from studies of ultrafine particles. Environ. Health Perspect. 113, 823–839.

Oukarroum, A., Bras, S., Perreault, F., Popovic, R., 2012. Inhibitory effects of silver nanoparticles in two green algae, Chlorella vulgaris and Dunaliella tertiolecta. Ecotoxicol. Environ. Saf. 78, 80–85.

Pan, Y., Neuss, S., Leifert, A., Fischler, M., Wen, F., Simon, U., Schmid, G., Brandau, W., Jahnen-Dechent, W., 2007. Size-dependent cytotoxicity of gold nanoparticles. Small 3, 1941–1949.

Park, M.V., Neigh, A.M., Vermeulen, J.P., de la Fonteyne, L.J., Verharen, H.W., Briedé, J.J., van Loveren, H., de Jong, W.H., 2011. The effect of particle size on the cytotoxicity, inflammation, developmental toxicity and genotoxicity of silver nanoparticles. Biomaterials 32, 9810–9817.

Roh, J.Y., Lee, J., Choi, J., 2006. Assessment of stress-related gene expression in the heavy metal-exposed nematode *Caenorhabditis elegans*: a potential biomarker for metal-induced toxicity monitoring and environmental risk assessment. Environ. Toxicol. Chem. 25, 2946–2956.

Roh, J.Y., Sim, S.J., Yi, J.H., Park, K.S., Chung, K.H., Ryu, D.Y., Choi, J., 2009. Ecotoxicity of silver nanoparticles on the soil nematode *Caenorhabditis elegans* using functional ecotoxicogenomics. Environ. Sci. Technol. 43, 3933–3940.

Shavandi, Z., Ghazanfari, T., Moghaddam, K.N., 2011. In vitro toxicity of silver nanoparticles on murine peritoneal macrophages. Immunopharmacol. Immunotoxicol. 33, 135–140.

Shoults-Wilson, W.A., Reinsch, B.C., Tsyusko, O.V., Bertsch, P.M., Lowry, G.V., Unrine, J.M., 2011. Effect of silver nanoparticle surface coating on bioaccumulation and reproductive toxicity in earthworm (*Eisenia fetida*). Nanotoxicology 5, 432–444.

Sung, J.H., Ji, J.H., Song, K.S., Lee, J.H., Choi, K.H., Lee, S.H., Yu, I.J., 2011. Acute inhalation toxicity of silver nanoparticles. Toxicol. Ind. Health 27, 149–154.

Tantra, R., Schulze, P., Quincey, P., 2010. Particuology Effect of nanoparticle concentration on zeta-potential measurement results and reproducibility. Particuology 8, 279–285.

Teodoro, J.S., Simões, A.M., Duarte, F.V., Rolo, A.P., Murdoch, R.C., Hussain, S.M., Palmeira, C.M., 2011. Assessment of the toxicity of silver nanoparticles in vitro: a mitochondrial perspective. Toxicol. In Vitro 25, 664–670.

Tiwari, D.K., Jin, T., Behari, J., 2011. Dose-dependent in-vivo toxicity assessment of silver nanoparticle in Wistar rats. Toxicol. Mech. Methods 21, 13–24.

van der Zande, M., Vandebriel, R.J., Van Doren, E., Kramer, E., Herrera Rivera, Z., Serrano-Rojero, C.S., Gremmer, E.R., Mast, J., Peters, R.J., Hollman, P.C., Hendriksen, P.J., Marvin, H.J., Peijnenburg, A.A., Bouwmeester, H., 2012. Distribution, elimination, and toxicity of silver nanoparticles and silver ions in rats after 28-day oral exposure. ACS Nano 6, 7427–7442.

Varaprasad, K., Mohan, Y.M., Vimala, K., Raju, K.M., 2011. Synthesis and characterization of hydrogel–silver nanoparticle-curcumin composites for wound dressing and antibacterial application. J. Appl. Polym. Sci. 8, 784–796.

Wu, Y., Zhou, Q., 2012. Dose- and time-related changes in aerobic metabolism, chorionic disruption, and oxidative stress in embryonic medaka (*Oryzias latipes*): underlying mechanisms for silver nanoparticle developmental toxicity. Aquat. Toxicol. 124–125, 238–246.

Yang, X., Gondikas, A.P., Marinakos, S.M., Auffan, M., Liu, J., Hsu-Kim, H., Meyer, J.N., 2012. Mechanism of silver nanoparticle toxicity is dependent on dissolved silver and surface coating in *Caenorhabditis elegans*. Environ. Sci. Technol. 46, 1119–1127.

Zhao, Y.L., Wu, Q.L., Li, Y.P., Wang, D.Y., 2013. Translocation, transfer, and in vivo safety evaluation of engineered nanomaterials in the non-mammalian alternative toxicity assay model of nematode *Caenorhabditis elegans*. RSC Adv. 3, 5741–5757.